
Variational Gaussian Processes with Signature Covariances

Csaba Toth
 Mathematical Institute
 University of Oxford
 t.g.csaba@gmail.com

Harald Oberhauser
 Mathematical Institute
 University of Oxford
 oberhauser@maths.ox.ac.uk

Abstract

We introduce a Bayesian approach to learn from stream-valued data by using Gaussian processes with the recently introduced signature kernel [20, 10] as covariance function. To cope with the computational complexity in time and memory that arises with long streams that evolve in large state spaces, we develop a variational Bayes approach with sparse inducing tensors. We provide an implementation based on GPFlow [11] and benchmark this variational Gaussian process model on supervised classification tasks for time series and text (a stream of words).

1 Introduction

For a given set \mathcal{X} , we call

Streams $(\mathcal{X}) := \{\mathbf{x} : \mathbf{x} = (t_i, x_i)_{i=1, \dots, \ell_{\mathbf{x}}}, (t_i, x_i) \in I \times \mathcal{X}, t_1 < \dots < t_{\ell_{\mathbf{x}}}, \ell_{\mathbf{x}} \in \mathbb{N}\}$

the set of *streams* in the *state space* \mathcal{X} with *index set* $I \subset [0, \infty)$; we call $\ell_{\mathbf{x}}$ the *length* of the stream $\mathbf{x} = (t_i, x_i)_{i=1, \dots, \ell_{\mathbf{x}}} \in \mathbf{Streams}(\mathcal{X})$. Classical examples that also appear in our benchmarks are

(multi-variate) time series $I = [0, \infty)$, $\mathcal{X} = \mathbb{R}^d$. The index set I represents time. Healthcare, economics, and engineering are a rich source of time series data.

text $I = \mathbb{N}$, $\mathcal{X} = \{A, B, \dots, Z, a, b, \dots, z, 1, 2, \dots, 9, 0\}$. The index set I set represents the position in the text, that is $t_i = i$ denotes the i th character in the text \mathbf{x} . Alternatively, $\mathcal{X} = \{\text{Aardvark}, \dots, \text{Zebra}\}$ are words and $t_i = i$ denotes the i th word in the text \mathbf{x} .

Learning from streams has received much attention from a wide range of scientific communities. Already for time series, the following issues occur in real-world data sets and have to be dealt with:

asynchronous sampling The observation grid (t_i) can change from instance to instance, i.e. for $\mathbf{x} = (t_i, x_i) \in \mathbf{Streams}(\mathcal{X})$ and $\mathbf{x}' = (t'_i, x'_i) \in \mathbf{Streams}(\mathcal{X})$, in general $(t_i)_i \neq (t'_i)_i$.

multi-modal different modes of activity can occur within an instance $\mathbf{x} = (t_i, x_i)$. Multi-modal in state means some coordinates evolve at different speed and scales; multi-modal in time means different time periods are governed by distinct regimes,

parametrization (ir-)relevance Many functions of streams, $f(\mathbf{x})$, are invariant to the parametrization, that is $f(\mathbf{x}) = f(\mathbf{x}^\rho)$ where $\mathbf{x}^\rho = (\rho(t_i), x_i)$ for an increasing function, *the time-change*, $\rho : I \equiv [0, \infty) \rightarrow [0, \infty)$; on the other hand, often parametrization is informative.

scalability Given a data set $\mathbf{X} = \{\mathbf{x}_1, \dots, \mathbf{x}_{n_{\mathbf{X}}}\} \subset \mathbf{Streams}(\mathcal{X})$ of $n_{\mathbf{X}}$ streams of maximal length $\ell_{\mathbf{X}} := \max_{\mathbf{x} \in \mathbf{X}} \ell_{\mathbf{x}}$ in a state space $\mathcal{X} = \mathbb{R}^d$, we have to be able to simultaneously cope with large $n_{\mathbf{X}}$, large $\ell_{\mathbf{X}}$, and large d .

Especially, the approach of identifying a time-series $\mathbf{x} = (t_i, x_i)$ as a large vector in $\mathbb{R}^{\ell_{\mathbf{x}}(1+d)}$ and subsequently applying a standard machine learning pipeline for vector-valued data can be troublesome; e.g. $\ell_{\mathbf{x}}$ or the grid (t_i) itself can vary sample-to-sample.

Contribution. In this paper, we provide a flexible and scalable Bayesian approach to learn from such streams by combining insights from stochastic analysis with Gaussian process models (GP, [31]). We first introduce a centered GP $f = (f_{\mathbf{x}})_{\mathbf{x} \in \text{Streams}(\mathcal{X})}$ with a covariance function given as the inner product of so-called signature features that describe a stream as a sequence of tensors [22]. This signature kernel was introduced in [20] and applied to frequentist kernel SVM classification of low-dimensional time series. We build on these results, but develop a sparse variational Bayes approach with tensors as inducing points. This yields a big speed up and ultimately allows us to learn from large data sets of long streams evolving in large state spaces, e.g. a time series in $\mathcal{X} = \mathbb{R}^{963}$ appears in our benchmarks. A methodological attractive property of this variational GP model (VGP) is that automatic relevance determination (ARD, [25, 29, 31]) can be used to proxy parametrization relevance in complete analogy to how ARD is applied to lengthscales. We provide a full implementation, based on GPFLOW [11] and Tensorflow, publically available at <https://github.com/tgcsaba/GPSig>. We benchmark this VGP on standard time-series classification tasks where it shows very strong performance and give a new application to text classification with word embeddings.

2 Gaussian priors for functions of streams

Functions of streams. The covariance function of a GP encodes the assumptions about the class of functions that we want to learn; in our setting this will be a large subset of $\mathbb{R}^{\text{Streams}(\mathcal{X})}$. The hyperparameters of the covariance function should be rich enough to impose further restrictions; e.g. we should be able to choose hyperparameters such that the Gaussian prior concentrates on the subset of functions that are invariant under reparametrization¹. Another issue is that many streams arise by discrete-time sampling of objects that evolve in continuous time, $\mathbf{x} = (t_i, x_i)_i$ with $x_i := x(t_i)$ for an object $(x(t))_{t \in [0, T]}$, $x(t) \in \mathcal{X}$ that evolves in continuous time and is observed at discrete times (t_i) . Hence, our GP model should have a well-defined limit as $\max_i |t_{i+1} - t_i| \downarrow 0$.

Streams as Paths. We address both issues—a large and structured function class and consistency in the high-frequency limit—by studying the problem in continuous time: firstly, we lift streams in \mathcal{X} to streams in a Hilbert space V by the mapping $\mathbf{x} = (t_i, x_i) \mapsto (t_i, \varphi_\theta(x_i))$, where $\varphi_\theta : \mathcal{X} \rightarrow V$ is a map parametrized by θ . Intuitively, φ_θ is a feature map for “static data” in \mathcal{X} . Secondly, we linearly interpolate between the points $(0, 0), (t_1, \varphi_\theta(x_1)), \dots, (t_{\ell_{\mathbf{x}}}, \varphi_\theta(x_{\ell_{\mathbf{x}}}))$ to go from discrete to continuous time. Put together, this defines a parametrized lift from streams to paths, $\varphi_\theta : \text{Streams}(\mathcal{X}) \rightarrow \text{Paths}(V)$, as

$$\varphi_\theta(\mathbf{x}) = \{t \mapsto ((t_{i+1} - t_i)^{-1} (\varphi_\theta(x_i)(t_{i+1} - t) + \varphi_\theta(x_{i+1})(t - t_i)))\}$$

where $\text{Paths}(V)$ denotes the space of continuous bounded variation paths of arbitrary length,

$$\text{Paths}(V) = \{\mathbf{x} \in \bigcup_{T>0} C([0, T], V) : \mathbf{x}(0) = 0, \|\mathbf{x}\|_1 < \infty\}$$

and $\|\mathbf{x}\|_1 := \sup_{0 \leq t_1 < \dots < t_n \leq T} \sum_i |x(t_{i+1}) - x(t_i)|_V$ denotes the bounded variation norm. This lift φ_θ can be modified to include more non-linearities, e.g. adding lags is a classic time-series pre-processing technique and justified by Taken’s theorem, [36], that guarantees that attractors in a high-dimensional dynamical system can be reconstructed from low-dimensional observations. In general, adding non-linearities is beneficial, [10, 20], but enlarges the state space V .

GPs for paths Any GP $g = (g_{\mathbf{x}})_{\mathbf{x} \in \text{Paths}(V)}$ induces a GP $f = (f_{\mathbf{x}})_{\mathbf{x} \in \text{Streams}(\mathcal{X})}$ via the pullback with φ_θ , that is, $f_{\mathbf{x}} := g_{\varphi_\theta(\mathbf{x})}$. Constructing a GP for path-valued data looks more daunting since the space of paths is even larger than the space of streams. However, a big advantage of working in continuous time is that we can rely on well-studied techniques from (stochastic) analysis. Concretely, we rely on the so-called signature map to represent a path faithfully in a graded manner as a sequence of tensors and this will give us a structured description of a large function space of streams. Another advantage of this “top-down” approach from continuous time to discrete time, is that it ensures—by construction—consistency in the high-frequency limit as streams approach paths.

¹We call $f \in \mathbb{R}^{\text{Streams}(\mathcal{X})}$ *invariant under reparametrization* if $f(\mathbf{x}) = f(\mathbf{y})$ for $\mathbf{x} = (t_i, x_i)$, $\mathbf{y} = (\rho(t_i), x_i)$ for any smooth increasing function $\rho : [0, \infty) \rightarrow [0, \infty)$.

Functions of paths. We first discuss the subset of functions of paths, $\mathcal{F}_{\text{inv}} \subset \mathbb{R}^{\text{Paths}(V)}$ that are *invariant under reparametrization*.² A natural candidate for \mathcal{F}_{inv} is the space

$$\{f \in \mathbb{R}^{\text{Paths}(V)} : f \text{ continuous and invariant under reparametrization}\}. \quad (1)$$

Unfortunately, it is hard to directly describe a useful and computationally tractable prior on this space. We therefore focus on a slightly smaller set of functions than (1), namely the set

$$\{f \in \mathbb{R}^{\text{Paths}(V)} : f \text{ continuous and invariant under tree-like equivalence}\} \quad (2)$$

by using an equivalence relation between paths, namely *tree-like equivalence*³. From an analytical point of view, tree-like invariances are more natural than reparametrization invariances—loosely speaking, tree-like equivalence between paths is analogous to Lebesgue almost sure equivalence between sets, see [15] for a detailed discussion. From a practical point of view, the difference between invariance under tree-like equivalence and under reparametrization is negligible and we invite the reader to use them as synonyms for the remainder of this article.

Functions of paths as linear functionals. A folk theorem from stochastic analysis guarantees that on compacts $K \subset \text{Paths}(V)$, the elements of (2) can be uniformly approximated by *linear functionals* of the so-called *signature*, see [22],

$$\forall \epsilon > 0 \exists w \in \bigoplus_{m \geq 0} V^{\otimes m} \text{ such that } \sup_{\mathbf{x} \in K} \|f(\mathbf{x}) - \langle w, \mathbf{S}(\mathbf{x}) \rangle\| < \epsilon. \quad (3)$$

The signature $\mathbf{S}(\mathbf{x}) = (\mathbf{S}_m(\mathbf{x}))_{m \geq 0} \in \prod_{m \geq 0} V^{\otimes m}$ is a sequence⁴ of tensors, recursively defined as

$$\mathbf{S}_m(\mathbf{x}) := \int_0^T dx^{\otimes m} := \int_0^T \left(\int_0^{T'} dx^{\otimes m-1} \right) \otimes dx_{T'}, \text{ and } \int_0^T dx_t^{\otimes 0} := 1.$$

Further, the map $\mathbf{x} \mapsto \mathbf{S}(\mathbf{x})$ is injective up to tree-like equivalence, that is $\mathbf{S}(\mathbf{x}) = \mathbf{S}(\mathbf{y})$ iff \mathbf{x} and \mathbf{y} are tree-like equivalent. This motivates our choice of function class⁵

$$\mathcal{F}_{\text{inv}} := \{g(\mathbf{x}) = \langle w, \mathbf{S}(\mathbf{x}) \rangle : w \in \bigoplus_{m \geq 0} V^{\otimes m}\} \subset \mathbb{R}^{\text{Paths}(V)}$$

since by (3), every function f in (2) can be arbitrary well approximated by elements of \mathcal{F}_{inv} . The big advantage of \mathcal{F}_{inv} is that priors on this set are given by priors on $w \in \bigoplus_{m \geq 0} V^{\otimes m}$. Hence, we define a centered GP $g = (g_{\mathbf{x}})_{\mathbf{x} \in \text{Paths}(V)}$ with covariance function

$$(\mathbf{x}, \mathbf{y}) \mapsto \mathbb{E}[g_{\mathbf{x}} g_{\mathbf{y}}] = \mathbb{E}_w[\langle w, \mathbf{S}(\mathbf{x}) \rangle \langle w, \mathbf{S}(\mathbf{y}) \rangle]. \quad (4)$$

In general, evaluating this covariance function is infeasible or at least computationally very costly. The existence of the covariance operator $C : V \rightarrow V$ such that (4) equals $(\mathbf{x}, \mathbf{y}) \mapsto \langle C \mathbf{S}(\mathbf{x}), \mathbf{S}(\mathbf{y}) \rangle$ follows from general principles. For priors with C trace-class and graded by $\sigma^2 = (\sigma_1^2, \dots, \sigma_m^2) \in \mathbb{R}^m$, (4) further simplifies to

$$(\mathbf{x}, \mathbf{y}) \mapsto \sum_{i=0}^m \sigma_i^2 \langle \mathbf{S}_i(\mathbf{x}), \mathbf{S}_i(\mathbf{y}) \rangle. \quad (5)$$

If V is a RKHS, the “*kernel trick*” from [20] can be modified to compute (5) without evaluating the signature maps $\mathbf{S}(\mathbf{x})$ and $\mathbf{S}(\mathbf{y})$ directly. Alternatively, if V is low-dimensional, (5) can be evaluated directly by first computing $\mathbf{S}(\mathbf{x})$ and $\mathbf{S}(\mathbf{y})$ and taking their inner product [32]. Both approaches—the kernel trick or the direct computation—already allow to apply this GP to some real-world data sets. However, the computational cost is prohibitive for many benchmarks, both in terms of running time and memory cost. Addressing this simply with low-rank approximations to the covariance matrix does usually not lead to effective GP methods, see [16] for a detailed discussion. In Section 3, we show that a variational Bayes approach can be combined with elementary tensor algebra. This yields massive speeds ups and benefits from the usual advantages of a variational approach.

²We call $f \in \mathbb{R}^{\text{Paths}(V)}$ *invariant under reparametrization* if $f(\mathbf{x}) = f(\mathbf{y})$ for $\mathbf{x} = (x_t)$, $\mathbf{y} = (x_{\rho(t)})$ for any smooth increasing function $\rho : [0, \infty) \rightarrow [0, \infty)$.

³We call $f \in \mathbb{R}^{\text{Paths}(V)}$ *invariant under tree-like equivalence* if $f(\mathbf{x}) = f(\mathbf{y})$ if \mathbf{x} is tree-like equiv. to \mathbf{y} .

⁴The direct product of vector spaces V_1, V_2, \dots is $\prod_{m \geq 0} V_m := \{(a_m)_{m \geq 0} : a_m \in V_m\}$. The direct sum $\bigoplus_{m \geq 0} V_m$ is the subset of sequences that have finitely many non-zero entries.

⁵If V is Hilbert, $\langle \cdot, \cdot \rangle_V$ extends canonically to $\prod_{m \geq 0} V^{\otimes m}$; set $\langle v_1 \otimes \dots \otimes v_m, w_1 \otimes \dots \otimes w_m \rangle := \prod_{i=1}^m \langle v_i, w_i \rangle_V$ and extend linearly to $\prod_{m \geq 0} V^{\otimes m}$. Thus every $w \in \bigoplus_{m \geq 0} V^{\otimes m} \subset \prod_{m \geq 0} V^{\otimes m}$ gives a linear functional $\langle w, \mathbf{S}(\mathbf{x}) \rangle$ of the signature $\mathbf{S}(\mathbf{x})$.

Parametrization ARD. We now consider the class of parameterization-variant functions of paths,

$$\{f \in \mathbb{R}^{\mathbf{Paths}(V)} : f \text{ continuous}\}. \quad (6)$$

Therefore we simply make the parametrization part of the trajectory in state space by defining the augmented state space $W := \mathbb{R} \oplus V$. We introduce a parameter $\tau \geq 0$ and the *augmented signature map* given as

$$\mathbf{S}^\tau(\mathbf{x}) := \mathbf{S}(\mathbf{x}^\tau) \text{ where } \mathbf{x}^\tau \in \mathbf{Paths}(W), \mathbf{x}^\tau(t) := (\tau \cdot t, \mathbf{x}(t)).$$

Then for any $\tau > 0$, $\mathbf{S}^\tau(\mathbf{x}) = \mathbf{S}^\tau(\mathbf{y})$ if and only if $\mathbf{x} = \mathbf{y}$. The same argument as above shows that

$$\mathcal{F} := \{g(\mathbf{x}) = \langle w, \mathbf{S}^\tau(\mathbf{x}) \rangle : w \in \bigoplus_{m \geq 0} W^{\otimes m}\} \subset \mathbb{R}^{\mathbf{Paths}(V)}$$

is dense, uniformly on compacts, in (6). We again consider a centered GP, $g = (g_{\mathbf{x}})_{\mathbf{x} \in \mathbf{Paths}(V)}$, but now with covariance function $(\mathbf{x}, \mathbf{y}) \mapsto \sum_{i=0}^m \sigma_i^2 \langle \mathbf{S}_i^\tau(\mathbf{x}), \mathbf{S}_i^\tau(\mathbf{y}) \rangle$ that has as an additional hyperparameter τ . This generalizes the covariance function (5), since for $\tau = 0$

$$\mathbf{S}^0(\mathbf{x}) = \mathbf{S}^0(\mathbf{y}) \text{ if and only if } \mathbf{x} \text{ and } \mathbf{y} \text{ are tree-like equivalent}$$

because all the additional signature coordinates, i.e. iterated integrals against the additional coordinate $t \mapsto \tau \cdot t$, are equal to 0. Hence $\langle \mathbf{S}^0(\mathbf{x}), \mathbf{S}^0(\mathbf{y}) \rangle = \langle \mathbf{S}(\mathbf{x}), \mathbf{S}(\mathbf{y}) \rangle$, and for $\tau > 0$, the centered GP on $\mathbf{Paths}(V)$ with covariance $\langle \mathbf{S}^\tau(\mathbf{x}), \mathbf{S}^\tau(\mathbf{y}) \rangle$ has a prior supported on $\mathcal{F} \subset \mathbb{R}^{\mathbf{Paths}(V)}$. As $\tau \downarrow 0$, the probability mass moves towards the subset $\mathcal{F}_{\text{inv}} \subset \mathcal{F}$, and with $\tau = 0$ all the mass lies in \mathcal{F}_{inv} .

A GP model for streams. Putting all the above together yields a centered GP $(f_{\mathbf{x}})_{\mathbf{x} \in \mathbf{Streams}(X)} \sim \mathcal{GP}(0, k)$ with covariance function

$$k_{\theta, \sigma^2, \tau}(\mathbf{x}, \mathbf{y}) = \sum_{i=0}^m \sigma_i^2 \langle \mathbf{S}_i^\tau \circ \varphi_\theta(\mathbf{x}), \mathbf{S}_i^\tau \circ \varphi_\theta(\mathbf{y}) \rangle. \quad (7)$$

This GP has hyperparameters (θ, σ^2, τ) : θ parametrizes the lift φ_θ from streams to paths; the vector $\sigma^2 = (\sigma_1^2, \dots, \sigma_m^2) \in [0, \infty)^m$ encodes the importance of the different tensor levels; finally $\tau \geq 0$ determines parametrization relevance. All these parameters can be determined by a model selection method from the data. This especially applies to the (non-)informativeness of parametrization by varying τ ; e.g. ARD can be used on τ , in the same way as for example ARD for length-scales in a RBF kernel. Prior knowledge is often available; e.g. for text the parametrization does not matter, thus $\tau \equiv 0$. In the supplementary material, we show that (7) is a natural generalization of the classical polynomial kernel for vector-valued data to stream-valued data.

3 GP classification with sparse variational inducing tensors

Given data (\mathbf{X}, Y) consisting of inputs $\mathbf{X} = (\mathbf{x}_1, \dots, \mathbf{x}_{n_{\mathbf{X}}})$ with labels $Y = (y_1, \dots, y_{n_{\mathbf{X}}})$, the task is to predict labels y_* of unseen points \mathbf{x}_* . A GP can be used as nuisance function to put a prior on the class membership probability by specifying $p(y = 1 | \mathbf{x}) = \sigma(f(\mathbf{x}))$ where σ is for example a sigmoid. Unfortunately, the resulting posterior class membership probability $p(y_* = 1 | \mathbf{x}_*, \mathbf{X}, Y)$ is non-tractable and classical approximations scale as $O(n_{\mathbf{X}}^3)$, see [31, Section 3.3]. This first led to *sparse* models, [30], that select a subset $\mathbf{Z} = \{\mathbf{z}_1, \dots, \mathbf{z}_{n_{\mathbf{Z}}}\}$ of \mathbf{X} consisting of $n_{\mathbf{Z}} \ll n_{\mathbf{X}}$ points, and subsequently to *pseudo-inputs*, [35], that selects points \mathbf{Z} that are not necessarily in \mathbf{X} . This was a big step towards complexity reduction, but pseudo-inputs are prone to overfitting, [26]. A different idea is to treat \mathbf{Z} as parameters of a variational approximation [37] and not as model parameters; that is the points \mathbf{Z} are chosen simultaneously with the hyperparameters of the GP by maximising a lower bound on the log-marginal likelihood $\log p(Y)$, the so-called *evidence lower bound* (ELBO). Initially applied to regression, it was extended to classification [8, 18]. Among its advantages are that it gives a nonparametric approximation to the true posterior, adding inducing points only improves the approximation, and any optimization method can be used to maximize the ELBO; see [27, 1, 7].

A canonical augmentation. Another idea is to go beyond the original index set and place inducing points \mathbf{Z} in a different space X' , that is, given a centered GP $g = (g_{\mathbf{x}})_{\mathbf{x} \in X}$ one augments the original index set X by a finite set X' to define a new GP $(g_{\mathbf{x}})_{\mathbf{x} \in X \cup X'}$ and then locates pseudo-inputs in this bigger model. This was suggested in [21] in the context of integral transforms and studied in more generality in [27]. In general, it is not clear how to find a useful augmentation set X' and define the new covariances. We make here the simple remark, that if the covariance is an inner product $k(\mathbf{x}, \mathbf{y}) := \langle \Phi(\mathbf{x}), \Phi(\mathbf{y}) \rangle$ with explicitly known⁶ Φ , then a natural augmentation is the “feature space” $X' = \text{span}\{\Phi(\mathbf{x}) : \mathbf{x} \in X\}$. The covariance function k of g can be simply extended to $X \cup X'$ by linearity, that is $k(\mathbf{x}, \mathbf{z}) := k(\mathbf{z}, \mathbf{x}) := \alpha k(\mathbf{x}, \mathbf{x}') + \beta k(\mathbf{x}, \mathbf{x}'')$ for $\mathbf{x} \in X$, $\mathbf{z} = \alpha\Phi(\mathbf{x}') + \beta\Phi(\mathbf{x}'') \in X'$, $\alpha, \beta \in \mathbb{R}$; analogous for $k(\mathbf{z}, \mathbf{z}')$ with $\mathbf{z}, \mathbf{z}' \in X'$.

Augmenting our GP model. For our GP model, $\Phi = \mathbf{S} \circ \varphi$ and $X' = \text{span}\{\Phi(\mathbf{x}) : \mathbf{x} \in \text{Streams}(X)\} \subset \prod_{m \geq 0} W^{\otimes m}$ are known in explicit form. This allows us to use both: pseudo-inputs by optimizing streams $\mathbf{Z} \subset \text{Streams}(X)$ and the augmentation by optimizing tensors $\mathbf{Z} \subset \prod_{m \geq 0} W^{\otimes m}$. Since the augmented method performed much better in our experiments, we only detail this tensor augmentation but note that the pseudo-input case follows similarly. Overfitting is a potential issue for the augmentation method, but the intuition is that the model remains marginally the same so variational inference in the augmented model and the original model should be comparable. For brevity, we set $\Phi_n(\mathbf{x}) := \mathbf{S}_n \circ \varphi(\mathbf{x}) \in W^{\otimes n}$. We use the inducing point locations

$$\mathbf{z} = (z_n)_{n=0, \dots, m} \in \prod_{n=0}^m W^{\otimes n} \text{ with } z_0 \in \mathbb{R} \text{ and } z_n = w_{n,1} \otimes w_{n,2} \otimes \dots \otimes w_{n,n} \text{ for } n \geq 1.$$

By the canonical extension of an inner product on W to an inner product on $\prod_{m \geq 0} W^{\otimes m}$, the covariance $\mathbb{E}[f_{\mathbf{z}} f_{\mathbf{z}'}]$ equals the inner product

$$\langle \mathbf{z}, \mathbf{z}' \rangle = \sum_{n=0}^m \langle z_n, z'_n \rangle = \sum_{n=0}^m \langle w_{n,1}, w'_{n,1} \rangle \langle w_{n,2}, w'_{n,2} \rangle \dots \langle w_{n,n}, w'_{n,n} \rangle. \quad (8)$$

The cross-covariance $\mathbb{E}[f_{\mathbf{x}} f_{\mathbf{z}}]$ equals the sum over n from 0 to m of the inner product

$$\begin{aligned} \langle \Phi_n(\mathbf{x}), z_n \rangle &= \left\langle \int_{0 < t_1 < t_2 < \dots < t_n < t_{\mathbf{x}}} d\varphi(x_{t_1}) \otimes \dots \otimes d\varphi(x_{t_n}), w_{n,1} \otimes \dots \otimes w_{n,n} \right\rangle \\ &= \int_{0 < t_1 < t_2 < \dots < t_n < t_{\mathbf{x}}} \langle d\varphi(x_{t_1}), w_{n,1} \rangle \dots \langle d\varphi(x_{t_n}), w_{n,n} \rangle, \end{aligned}$$

again by linearity of integration and the inner product. Finally, φ maps streams to piecewise linear paths and for such paths the integrals reduce to sums, hence $\langle \Phi_n(\mathbf{x}), z_n \rangle$ equals

$$\sum_{1 \leq i_1 \leq \dots \leq i_n \leq t_{\mathbf{x}}} c(i_1, \dots, i_m) \langle \varphi(x_{i_1+1}) - \varphi(x_{i_1}), w_{n,1} \rangle \dots \langle \varphi(x_{i_n+1}) - \varphi(x_{i_n}), w_{n,n} \rangle \quad (9)$$

for an explicitly known function $c(i_1, \dots, i_m) \leq 1$. A direct calculation shows that replacing $c(i_1, \dots, i_m)$ with 1 if there are no repeating indices in (i_1, \dots, i_m) and otherwise with 0 gives a good approximation⁷ to (9) but makes the recursive algorithms simpler. Below we use this approximation to (9) but note that a simple modification exactly computes (9) for a marginal computational overhead.

Algorithms. We need to compute covariances between: (i) tensors and tensors, (ii) streams and tensors, (iii) streams and streams. We give vectorized algorithms for (i) and (ii) in Algorithms 1 and 2, respectively. In the supplementary material we give the algorithm for (iii), which is a modification of algorithm 3 from [20]. To start off with, assume that the required memory for $v \in W$ is $O(d)$, and that it takes $O(c)$ time to compute the inner product $\langle v, v' \rangle$ for $v, v' \in W$. If $n_{\mathbf{Z}}$ denotes the number of inducing points, the memory required to store the location tensors is $O(n_{\mathbf{Z}} \cdot m^2 \cdot d)$, where m is the truncation degree for the signature map. In our experiments, m was learnt from the data to be $m \leq 5$ in most cases, the order of a constant. Therefore, the memory contribution of these inducing tensors is considerably less compared to the learning inputs, which are stored in $O(n_{\mathbf{X}} \cdot l_{\mathbf{X}} \cdot d)$

⁶Mercer’s Theorem guarantees the existence of Φ , but not in explicit form.

⁷It converges to $\langle \Phi(\mathbf{x}), \mathbf{z} \rangle$ when the grid gets finer, $|t_{i+1} - t_i| \downarrow 0$, see also [22, 20, 15].

memory, denoting $n_{\mathbf{X}}$ and $l_{\mathbf{X}}$ the number and maximal length of streams. This is important because the inducing tensors are variational parameters, and not amenable to subsampling, while the learning inputs can be subsampled as noted by [18]. When memory is a bottleneck, as for GPUs, such memory savings are decisive. A backward pass through the algorithms to compute gradients requires to keep all intermediate values of the forward pass to be stored, therefore, computations on the fly do not further reduce the footprint. Algorithms 1 and 2 implement formulas (8) and (9) by vectorized computation using arrays. For an array, we define Σ as the slice-wise sum operator, \boxplus as the (forward) cumulative sum operator, $+1$ as the shift operator, where elements outside the bounds of an array are treated as zeroes, as opposed to rolling around elements, and \odot denotes the element-wise product of arrays. Since these are standard operations in computing, we refer for their formal definition to the supplementary material.

Algorithm 1: Evaluation of the tensor-tensor covariance matrix $K_{\mathbf{ZZ}} = (\mathbb{E}[f_{\mathbf{z}} f_{\mathbf{z}'}])_{\mathbf{z}, \mathbf{z}' \in \mathbf{Z}}$

Data: Inducing tensors $\mathbf{Z} = \{\mathbf{z}_1, \dots, \mathbf{z}_{n_{\mathbf{Z}}}\} \subset \prod_{n=0}^m W^{\otimes n}$, grading vector $\sigma^2 = [\sigma_0^2, \sigma_1^2, \dots, \sigma_m^2]$

Result: Covariance matrix of inducing points $K_{\mathbf{ZZ}}$

- 1: Compute an $(n_{\mathbf{Z}} \times n_{\mathbf{Z}} \times m \times \star)$ -array K such that $K[i, j|n] = \left[\langle w_{n,k}^i, w_{n,k}^j \rangle \right]_{k=1, \dots, n}$ for $i, j \in \{1, \dots, n_{\mathbf{Z}}\}$ and $n \in \{1, \dots, m\}$
 - 2: Initialize R an $(n_{\mathbf{Z}} \times n_{\mathbf{Z}})$ constant array of σ_0^2
 - 3: **for** $n = 1$ to m **do**
 - 4: Set $A \leftarrow K[:, :, |n, 1]$
 - 5: **for** $k = 2$ to m **do**
 - 6: Iterate $A \leftarrow K[:, :, |n, k] \odot A$
 - 7: **end**
 - 8: Update $R \leftarrow R + \sigma_n^2 \cdot A$
 - 9: **end**
 - 10: Return R
-

Algorithm 1 computes the covariance matrix $K_{\mathbf{ZZ}}$ of $n_{\mathbf{Z}}$ inducing points in $O(n_{\mathbf{Z}}^2 \cdot m^2 \cdot c)$ time. Additionally to storing the inducing tensors, the total memory required is of $O(n_{\mathbf{Z}}^2 \cdot m^2)$.

Algorithm 2: Evaluation of the stream-tensor covariance matrix $K_{\mathbf{XZ}} = (\mathbb{E}[f_{\mathbf{x}} f_{\mathbf{z}}])_{\mathbf{x} \in \mathbf{X}, \mathbf{z} \in \mathbf{Z}}$

Data: Streams $\mathbf{X} = \{\mathbf{x}_1, \dots, \mathbf{x}_{n_{\mathbf{X}}}\} \subset \text{Streams}(W)$, inducing tensors

$\mathbf{Z} = \{\mathbf{z}_1, \dots, \mathbf{z}_{n_{\mathbf{Z}}}\} \subset \prod_{n=0}^m W^{\otimes n}$, grading vector $\sigma^2 = (\sigma_0^2, \sigma_1^2, \dots, \sigma_m^2)$

Result: Cross-covariance matrix $K_{\mathbf{XZ}}$ between the GP evaluations and the inducing points

- 1: Compute an $(n_{\mathbf{X}} \times n_{\mathbf{Z}} \times (l_{\mathbf{X}} - 1) \times m \times \star)$ -array K s.t. $K[i, j|l, n] = \left[\langle \Delta x_{i, t_l}, w_{n,k}^j \rangle \right]_{k=1, \dots, n}$ with $i \in \{1, \dots, n_{\mathbf{X}}\}$, $j \in \{1, \dots, n_{\mathbf{Z}}\}$, $l \in \{1, \dots, l_{\mathbf{X}} - 1\}$, $n \in \{1, \dots, m\}$
 - 2: Initialize an $(n_{\mathbf{X}} \times n_{\mathbf{Z}})$ array R with constants σ_0^2
 - 3: **for** $n = 1$ to m **do**
 - 4: Assign $A \leftarrow K[:, :, |:, n, 1]$
 - 5: **for** $k = 2$ to m **do**
 - 6: Iterate $A \leftarrow K[:, :, |:, n, k] \odot A[:, :, |\boxplus + 1]$
 - 7: **end**
 - 8: Update $R \leftarrow R + \sigma_n^2 \cdot A[:, :, |\Sigma]$
 - 9: **end**
 - 10: Return R
-

Algorithm 2 computes the cross-covariance matrix $K_{\mathbf{XZ}}$ between $(f_{\mathbf{x}_i})_{i=1, \dots, n_{\mathbf{X}}}$ and $(f_{\mathbf{z}_i})_{i=1, \dots, n_{\mathbf{Z}}}$ in $O(n_{\mathbf{X}} \cdot n_{\mathbf{Z}} \cdot m^2 \cdot l_{\mathbf{X}} \cdot c)$ time. Since this is linear in the maximal length $l_{\mathbf{X}}$ of streams, it can be evaluated efficiently. Algorithm 2 requires an additional $O(n_{\mathbf{X}} \cdot n_{\mathbf{Z}} \cdot l_{\mathbf{X}} \cdot m^2)$ memory. This is again linear in $l_{\mathbf{X}}$ and can be further decreased by tuning $n_{\mathbf{X}}$, the batch size in the optimization procedure.

4 Benchmarks

For our VGP for streams we can use pseudo-inputs, augmentation, and low-rank approximations (that is, in every optimization step a low-rank approximation to $K_{\mathbf{x}\mathbf{x}}$ is computed in linear time in $l_{\mathbf{x}}$) for variational inference. We implemented all three in Python [19] using GPFLOW [11] and Tensorflow, see <https://github.com/tgcsaba/GPSig>; all data sets used are publically available. The experiments were run on a standard notebook connected to a single nVidia 1080 Ti GPU. To learn the variational parameters and the hyperparameters of the kernel, we use stochastic variational inference [17] with a Nadam optimizer [13], that showed superior performance to other SGD variants in our experiments. The optimization procedure must be carefully fine-tuned to reduce the variance across different runs.⁸ We use two different RKHS V on \mathbb{R}^d : one given by an Euclidean (linear) kernel, the other by an RBF kernel. We call the resulting models GPSigLin and GPSigRBF.

Task 1: multi-variate time series classification. Time series are streams with $\mathcal{X} = \mathbb{R}^d$ and index set $I = [0, \infty)$. We benchmark on the collection [2] of multivariate time series. As usual, we report as baseline 1-nearest neighbours with dynamic time warping distance computed as the sum of distances between the corresponding univariate time series and each dimension is z-normalized (DTW). We also report accuracies of two recent, state-of-the-art methods, SMTS [3] and mvARF [38]. The reported accuracies of STMS and mvARF are acquired from the respective publications to avoid bias in setting parameters, etc.; DTW accuracies are also taken from [3, 4].

Table 1: Datasets [2, 24] for task 1 and task 2

Name	classes	dimension	length	train cases	test cases
Arabic Digits	10	13	4–93	6600	2200
AUSLAN	95	22	345–136	1140	1425
Character Traj.	20	3	60–182	300	2558
CMU MOCAP	2	62	127–580	29	29
ECG	2	2	39–152	100	100
Jap. Vowels	9	12	7–29	270	370
Kick vs Punch	2	62	274–841	16	10
LIBRAS	15	2	45	360	180
PEMS	7	963	144	267	173
PenDigits	10	2	8	300	10692
Uwave	8	3	315	896	4278
Walk vs Run	2	62	128–1918	28	896
Wafer	2	6	104–198	298	896
IMDB	2	300	35–120	2000	1000

Task 2: text classification. Texts are streams with $\mathcal{X} = \text{Words} = \{\text{Aardvark}, \dots, \text{Zebra}\}$ and index set $I = \mathbb{N}$. We use the collection [24] of IMDB movie reviews labelled with positive or negative sentiment. We removed stop-words from 3000 randomly selected reviews of length 35–120 for training. As baseline, we tested different classifiers using bag-of-words features, namely an XGBoost classifier (BW+XGB), a VGP with an order agnostic linear kernel (BW+GPLin), and a VGP with an order agnostic RBF kernel (BW+GPRBF). For BW+XGB, we learned the parameters $n_{\text{estimators}} = [10, 100, 1000]$ and $max_{\text{depth}} = [3, 5, 10]$ via 3-fold CV on the training set, the parameters of the GPs were learnt by ARD. While this is not a state-of-the-art LSTM method, it is a competitive baseline. Our GP model $(f_{\mathbf{x}})_{\mathbf{x} \in \text{Streams}(\text{Words})}$, uses a pretrained word2vec model⁹ as static feature map $\varphi : \text{Words} \rightarrow \mathbb{R}^{300}$ and we set $\tau = 0$ since the information in text is invariant to reading speed.

⁸Following [1], we train with fixed hyperparameters for the first n iterations (typically $n = 1000$) to tighten the ELBO. Then, we unfix the kernel hyperparameters and use a learning rate schedule where we start small (typically 1×10^{-3}) and gradually increase it to a maximum value (typically 1×10^{-2}), train until the optimizer is finished exploring the space, and gradually decrease it again to drive the optimizer to settle at the closest local optima. Since hyperparameters of VGPs are sensitive to initialization, we jointly normalized all streams with the maximum absolute value of each feature dimension using a truncated distribution at the (5, 95) percentiles. We found it is beneficial to initialize the kernel constants to 0: $\sigma = (\sigma_0, \sigma_1, \dots, \sigma_m) = (0, 1, \dots, 1)$.

⁹See [28] and <https://code.google.com/archive/p/word2vec/>

Table 2: Classification accuracies on test sets

Task 1	GPSigLin	GPSigRBF	DTW	SMTS	mvARF
Arabic Digits	0.972 \pm 0.002	0.983 \pm 0.002	0.908	0.964	0.952
AUSLAN	0.981 \pm 0.005	0.967 \pm 0.009	0.762	0.947	0.934
Character Traj.	0.961 \pm 0.003	0.970 \pm 0.005	0.967	0.992	0.928
CMU MOCAP	1.000 \pm 0.000	1.000 \pm 0.000	0.931	0.997	1.000
ECG	0.828 \pm 0.024	0.826 \pm 0.013	0.850	0.818	0.785
Jap. Vowels	0.894 \pm 0.004	0.983 \pm 0.003	0.649	0.969	0.959
Kick vs Punch	0.900 \pm 0.070	0.940 \pm 0.054	0.900	0.820	0.976
Libras	0.833 \pm 0.007	0.921 \pm 0.009	0.800	0.909	0.945
PEMS	0.809 \pm 0.014	0.937 \pm 0.035	0.832	NA	NA
PenDigits	0.951 \pm 0.001	0.955 \pm 0.001	0.925	0.917	0.923
Uwave	0.951 \pm 0.001	0.956 \pm 0.002	0.929	0.941	0.952
Walk vs Run	1.000 \pm 0.000	1.000 \pm 0.000	1.000	1.000	1.000
Wafer	0.977 \pm 0.003	0.974 \pm 0.004	0.960	0.965	0.931
Task 2	GPSigLin	GPSigRBF	BW+GPLin	BW+GPRBF	BW+XG
IMDB	0.838 \pm 0.003	0.820 \pm 0.004	0.817	0.818	0.826

Results. Table 2 shows the accuracies. For our VGP models (GPSigRBF, GPSigLin) we report the best of pseudo-input, augmentation, and low-rank method. In fact, the augmentation performed overall the best, except on two datasets where it was beaten by the low-rank method. Pseudo-inputs were not competitive. For time-series classification, our VGP performs very well and we note that it, like all GPs classifiers, also provides the posterior class membership probability with a variance of the estimate unlike some of the other state-of-the-art methods. Our algorithms conserve memory, which makes the use of GPUs possible; e.g. PEMS is often left out of benchmarks since the high dimension $d = 963$ is an issue for many methods; training our model on PEMS took less than 25 minutes, testing is a matter of seconds. A disadvantage of our VGP for streams is its sensitivity to initialization of the optimizer. This is a general drawback of VGPs [1], but we note that the variance in our results is very low due to carefully tuned optimization settings.

5 Conclusion and Future work

Signatures are classical objects in stochastic analysis but their use in machine learning is more recent [22, 23, 39, 40, 10, 20, 32, 5]. Their use in Bayesian inference is unexplored. Our model relies on previous results on signature kernels [20], but the variational approach with sparse tensors is essential to deal with large sets of long streams evolving in high-dimensional state spaces. Besides its strong performance on standard benchmarks, we believe that its most attractive property is that it puts a well-known insight from the engineering community about the importance of parametrization-invariance into a principled probabilistic model selection approach. This paper is a small step towards a general Bayesian methodology and many follow up questions arise. On a theoretical level, our GP is indexed by a set that is not even locally compact which is in stark contrast to the usual case of vector-valued data. Consistency of Bayesian procedures [12, 14] is already a subtle topic for GPs indexed by vectors and the methods in [10, 34] might be useful to address such questions. Further, the GP augmentation via the feature space proposed in Section 3 can be carried out for other GPs, as long as feature map and feature space are known explicitly. The approaches [27, 33] via stochastic process divergence provide an elegant framework to study this canonical augmentation further. On a more applied level, an important question is how to update the inference procedure online as streams get longer. This is a surprisingly little studied topic and we refer to [6] for recent progress. The text experiment indicates that signatures have potential in NLP: our text classifier only marginally beats BW, but it does this by capturing very different information, namely the order information in a sequence of words unlike word order agnostic BW. Our other benchmarks focus on time-series classification since this is a well-studied topic with very strong baselines that allow for a fair comparison. However, we emphasize that streams do not need to be indexed by a set that represents “time” as the text example shows, and we point to persistence paths of barcodes [9] in topological data analysis as another interesting source of such streams.

References

- [1] Matthias Bauer, Mark van der Wilk, and Carl Edward Rasmussen. Understanding probabilistic sparse Gaussian process approximations. In *Advances in neural information processing systems*, pages 1533–1541, 2016.
- [2] Mustafa Baydogan. *Multivariate Time Series Classification Datasets*, 2015. [Accessed: 2019-05-13].
- [3] Mustafa Gokce Baydogan and George Runger. Learning a symbolic representation for multivariate time series classification. *Data Mining and Knowledge Discovery*, 29(2):400–422, 2015.
- [4] Mustafa Gokce Baydogan and George C. Runger. Time series representation and similarity based on local autopatterns. *Data Mining and Knowledge Discovery*, 30:476–509, 2015.
- [5] Patric Bonnier, Patrick Kidger, Imanol Perez Arribas, Christopher Salvi, and Terry Lyons. Deep signatures. *CoRR*, abs/1905.08494, 2019.
- [6] Thang D Bui, Cuong Nguyen, and Richard E Turner. Streaming sparse Gaussian process approximations. In *Advances in Neural Information Processing Systems*, pages 3299–3307, 2017.
- [7] Thang D. Bui, Josiah Yan, and Richard E. Turner. A Unifying Framework for Gaussian Process Pseudo-Point Approximations using Power Expectation Propagation. *Journal of Machine Learning Research*, 18(104):1–72, 2017.
- [8] Kian Ming A Chai. Variational multinomial logit Gaussian process. *Journal of Machine Learning Research*, 13(Jun):1745–1808, 2012.
- [9] Ilya Chevyrev, Vidit Nanda, and Harald Oberhauser. Persistence Paths and Signature Features in Topological Data Analysis. *IEEE Transactions on Pattern Analysis and Machine Intelligence*, pages 1–1, 2018.
- [10] Ilya Chevyrev and Harald Oberhauser. Signature moments to characterize laws of stochastic processes. *arXiv preprint 1810.10971*, 2018.
- [11] Alexander G. de G. Matthews, Mark van der Wilk, Tom Nickson, Keisuke Fujii, Alexis Boukouvalas, Pablo León-Villagrà, Zoubin Ghahramani, and James Hensman. Gpflow: A gaussian process library using tensorflow. *Journal of Machine Learning Research*, 18:40:1–40:6, 2017.
- [12] Persi Diaconis, David Freedman, et al. On the consistency of Bayes estimates. *The Annals of Statistics*, 14(1):1–26, 1986.
- [13] Timothy Dozat. Incorporating Nesterov Momentum into Adam. 2015.
- [14] Peter Grünwald and John Langford. Suboptimal behavior of Bayes and MDL in classification under misspecification. *Machine Learning*, 66(2-3):119–149, 2007.
- [15] Ben Hambly and Terry Lyons. Uniqueness for the Signature of a path of bounded variation and the reduced path group. *Ann. of Math. (2)*, 171(1):109–167, 2010.
- [16] James Hensman, Alexander G. de G. Matthews, and Zoubin Ghahramani. Scalable variational Gaussian Process Classification. In *AISTATS*, 2015.
- [17] James Hensman, Nicolás Fusi, and Neil D. Lawrence. Gaussian processes for big data. *CoRR*, abs/1309.6835, 2013.
- [18] James Hensman, Alexander Matthews, and Zoubin Ghahramani. Scalable variational Gaussian process classification. 2015.
- [19] Eric Jones, Travis Oliphant, Pearu Peterson, et al. SciPy: Open source scientific tools for Python, 2001–.
- [20] Franz J. Kiraly and Harald Oberhauser. Kernels for sequentially ordered data. *Journal of Machine Learning Research*, 20(31):1–45, 2019.
- [21] Miguel Lázaro-Gredilla and Anibal Figueiras-Vidal. Inter-domain Gaussian processes for sparse inference using inducing features. In *Advances in Neural Information Processing Systems*, pages 1087–1095, 2009.

- [22] Terry Lyons. Rough paths, signatures and the modelling of functions on streams. In *Proceedings of the International Congress of Mathematicians*, 2014.
- [23] Terry Lyons, Hao Ni, and Harald Oberhauser. A feature set for streams and an application to high-frequency financial tick data. In *BigDataScience '14*, 2014.
- [24] Andrew L. Maas, Raymond E. Daly, Peter T. Pham, Dan Huang, Andrew Y. Ng, and Christopher Potts. Learning word vectors for sentiment analysis. In *Proceedings of the 49th Annual Meeting of the Association for Computational Linguistics: Human Language Technologies - Volume 1*, HLT '11, pages 142–150, Stroudsburg, PA, USA, 2011. Association for Computational Linguistics.
- [25] David JC MacKay. Bayesian nonlinear modeling for the prediction competition. *ASHRAE transactions*, 100(2):1053–1062, 1994.
- [26] Alexander G de G Matthews. *Scalable Gaussian process inference using variational methods*. PhD thesis, Cambridge University, 2017.
- [27] Alexander G de G Matthews, James Hensman, Richard Turner, and Zoubin Ghahramani. On sparse variational methods and the Kullback-Leibler divergence between stochastic processes. *Journal of Machine Learning Research*, 51:231–239, 2016.
- [28] Tomas Mikolov, Kai Chen, Gregory S. Corrado, and Jeffrey Dean. Efficient estimation of word representations in vector space. *CoRR*, abs/1301.3781, 2013.
- [29] Radford M Neal. *Bayesian learning for neural networks*, volume 118. Springer Science & Business Media, 2012.
- [30] Joaquin Quiñero-Candela and Carl Edward Rasmussen. A unifying view of sparse approximate Gaussian process regression. *Journal of Machine Learning Research*, 6(Dec):1939–1959, 2005.
- [31] Carl Edward Rasmussen and Christopher KI Williams. Gaussian processes for machine learning. 2006. *The MIT Press, Cambridge, MA, USA*, 38:715–719, 2006.
- [32] Jeremy Reizenstein and Benjamin Graham. The iisignature library: efficient calculation of iterated-integral signatures and log signatures. *CoRR*, abs/1802.08252, 2018.
- [33] Matthias Seeger. Pac-bayesian generalisation error bounds for gaussian process classification. *Journal of machine learning research*, 3(Oct):233–269, 2002.
- [34] Carl-Johann Simon-Gabriel and Bernhard Schölkopf. Kernel distribution embeddings: Universal kernels, characteristic kernels and kernel metrics on distributions. *Journal of Machine Learning Research*, 19(44):1–29, 2018.
- [35] Edward Snelson and Zoubin Ghahramani. Sparse Gaussian processes using pseudo-inputs. In *Advances in neural information processing systems*, pages 1257–1264, 2006.
- [36] Floris Takens. Detecting strange attractors in turbulence. In *Dynamical systems and turbulence, Warwick 1980*, pages 366–381. Springer, 1981.
- [37] Michalis Titsias. Variational learning of inducing variables in sparse Gaussian processes. In *Artificial Intelligence and Statistics*, pages 567–574, 2009.
- [38] Kerem Sinan Tuncel and Mustafa Gokce Baydogan. Autoregressive forests for multivariate time series modeling. *Pattern Recognition*, 73:202–215, 2018.
- [39] Weixin Yang, Lianwen Jin, Hao Ni, and Terry Lyons. Rotation-free online handwritten character recognition using dyadic path signature features, hanging normalization, and deep neural network. *2016 23rd International Conference on Pattern Recognition (ICPR)*, pages 4083–4088, 2016.
- [40] Weixin Yang, Lianwen Jin, Dacheng Tao, Zecheng Xie, and Ziyong Feng. Dropsample: A new training method to enhance deep convolutional neural networks for large-scale unconstrained handwritten chinese character recognition. *Pattern Recognition*, 58:190–203, 2016.

6 Supplementary material

In the supplementary material we give (a) more background and intuition about signatures, (b) formal definitions of the notation used in Algorithms 1 and 2, (c) an algorithm used for computing the covariance matrix between streams and streams, (d) a more detailed discussion of our benchmarks and the optimization procedure.

6.1 Signatures as generalized monomials

Signature might be unfamiliar to most people in machine learning, but we emphasize that the signature of the path is simply a sequence of tensors. To gain intuition, we discuss the case of paths in a finite dimensional state space $V = \mathbb{R}^d$. Recall that the signature $\mathbf{S}(\mathbf{x}) = (\mathbf{S}_m(\mathbf{x}))_{m \geq 0}$ is the sequence of tensors $\mathbf{S}_m(\mathbf{x})$ that are defined as iterated integrals, that is

$$\mathbf{S}_m(\mathbf{x}) = \int_0^T \int_0^{t_{m-1}} \cdots \int_0^{t_2} dx(t_1) \otimes \cdots \otimes dx(t_m) \in (\mathbb{R}^d)^{\otimes m}.$$

One can just spell this out in coordinates, that is, if we denote $\mathbf{x} = (x^1(t), \dots, x^d(t))_{t \in [0, T]}$ then the $(i_1, \dots, i_m) \in \{1, \dots, d\}^m$ -coordinate of the tensor $\mathbf{S}_m(\mathbf{x})$ equals

$$\mathbf{S}_m^{i_1, \dots, i_m}(\mathbf{x}) = \int_0^T \int_0^{t_{m-1}} \cdots \int_0^{t_2} dx^{i_1}(t_1) \cdots dx^{i_m}(t_m).$$

Since the iterated integrals are defined in Riemann–Stieljes sense this equals

$$\mathbf{S}_m^{i_1, \dots, i_m}(\mathbf{x}) = \int_0^T \int_0^{t_{m-1}} \cdots \int_0^{t_2} \dot{x}^{i_1}(t_1) \cdots \dot{x}^{i_m}(t_m) dt_1 \cdots dt_m \in \mathbb{R}$$

where $\dot{x}^i(t)$ denotes the time derivative of $x^i(t)$ (which exists for bounded variation paths for almost every t). In general, these iterated integrals can be calculated by any numerical integration scheme but for the important case when the path \mathbf{x} is piecewise linear—which arises when we lift streams to paths via φ_θ —a direct calculation shows that these iterated integrals reduce to iterated sums of path increments. Much more is known about signatures and how they represent paths and we refer to [22] for further references.

It is instructive to regard the signature map

$$\mathbf{Paths}(\mathbb{R}^d) \ni \mathbf{x} \mapsto (\mathbf{S}_m(\mathbf{x}))_{m \geq 0} \in \prod_{m \geq 0} (\mathbb{R}^d)^{\otimes m}$$

as a generalization of the moment map

$$\mathbb{R}^d \ni \mathbf{x} \mapsto \left(\frac{\mathbf{x}^{\otimes m}}{m!} \right)_{m \geq 0} \in \prod_{m \geq 0} (\mathbb{R}^d)^{\otimes m}$$

from the domain of vectors \mathbb{R}^d to the domain of paths $\mathbf{Paths}(\mathbb{R}^d)$. Indeed, for a linear path $\mathbf{x} \in \mathbf{Paths}(\mathbb{R}^d)$, given as $\mathbf{x}_t = t \cdot v$ for a $v \in \mathbb{R}^d$, a direct calculation shows the m -th iterated integral is $\mathbf{S}_m(\mathbf{x}) = \frac{v^{\otimes m}}{m!}$. From this point of view of signatures as monomials, the GP $(g_{\mathbf{x}})_{\mathbf{Paths}(\mathbb{R}^d)}$ indexed by $\mathbf{Paths}(\mathbb{R}^d)$ with the signature covariance in Section 2 can now be simply identified as a generalization of a GP $(g'_{\mathbf{x}})_{\mathbf{x} \in \mathbb{R}^d}$ indexed by \mathbb{R}^d with the inhomogeneous polynomial kernel as covariance, see [31, Section 2.2]: with $(\sigma_0^2, \dots, \sigma_m^2) = (1, \dots, 1)$ and piecewise linear paths \mathbf{x}, \mathbf{y} the signature kernel (5) equals $(1 + c \cdot \langle v_1, v_2 \rangle_{\mathbb{R}^d})^m$ with $c = (m!)^2$ since $\mathbf{S}(\mathbf{x}) = \left(\frac{v_1^{\otimes m}}{m!} \right)$ and $\mathbf{S}(\mathbf{y}) = \left(\frac{v_2^{\otimes m}}{m!} \right)$.

6.2 Notation for array computations.

We define notation based on [20] for concisely describing vectorized computations. Let A and B be k -fold arrays of size $(n_1 \times n_2 \times \cdots \times n_k)$, indexed by $i_j \in \{1, 2, \dots, n_j\}$ for $j \in \{1, 2, \dots, k\}$. For semantic purposes, we equivalently denote the element of A at the index (i_1, i_2, \dots, i_k) by $A[i_1, i_2, i_3, \dots, i_k]$ and $A[\bar{i}_1, \bar{i}_2 | \bar{i}_3, \dots, \bar{i}_k]$, that is, we interchangeably use commas and bars to delimit indices, with the latter used to separate semantically distinct group of indices for transparency. Then, we define the following operations.

(i) The cumulative sum along axis j defined as:

$$A[:, \dots, :, \boxplus, :, \dots, :][i_1, \dots, i_{j-1}, i_j, i_{j+1}, \dots, i_k] := \sum_{\kappa=1}^{i_j} A[i_1, \dots, i_{j-1}, \kappa, i_{j+1}, \dots, i_k].$$

(ii) The slice-wise sum along axis j as

$$A[:, \dots, :, \Sigma, :, \dots, :][i_1, \dots, i_{j-1}, i_{j+1}, \dots, i_k] := \sum_{\kappa=1}^{n_j} A[i_1, \dots, i_{j-1}, \kappa, i_{j+1}, \dots, i_k].$$

(iii) The shift along axis j by $+m$ for a positive integer m as

$$A[:, \dots, :, +m, :, \dots, :][i_1, \dots, i_j, \dots, i_k] := \begin{cases} A[i_1, \dots, i_j - m, \dots, i_k], & \text{if } i_j > m, \\ 0, & \text{if } i_j \leq m. \end{cases}$$

(iv) The element-wise product of arrays A and B is defined as

$$A \odot B[i_1, \dots, i_k] = A[i_1, \dots, i_k] \cdot B[i_1, \dots, i_k].$$

Additionally, note that the use of the cumulative sum, \boxplus , in conjunction with the shift by 1 operator, $+1$, along the same axis is equivalent to an exclusive cumulative sum, where in the new array the i_j th index contains the sum of the original array's elements from 1 to $i_j - 1$.

6.3 Computing the stream vs stream covariance matrix.

To compute GP predictions at unseen data points, one needs to compute the covariances between the input streams. As mentioned in Section 3 this follows by simple modification of Algorithm 3 in [20] but for convenience of the reader we give it in detail. We assume that we have $n_{\mathbf{X}}$ streams, each of length $l_{\mathbf{X}}$, for streams of different length, just repeating observations as required, due to the parametrization invariance of signatures.

Algorithm 3: Computing the stream-stream covariance matrix $K_{\mathbf{X}\mathbf{X}} = (\mathbb{E}[f_{\mathbf{x}} f_{\mathbf{x}'}])_{\mathbf{x}, \mathbf{x}' \in \mathbf{X}}$

Data: Streams $\mathbf{X} = \{\mathbf{x}_1, \dots, \mathbf{x}_{n_{\mathbf{X}}}\} \subset \mathbf{Streams}(W)$, grading vector $\sigma^2 = (\sigma_0^2, \sigma_1^2, \dots, \sigma_m^2)$

Result: Covariance matrix $K_{\mathbf{X}\mathbf{X}}$ between the GP evaluations

- 1: Compute an $(n_{\mathbf{X}} \times n_{\mathbf{X}} \times (l_{\mathbf{X}} - 1) \times (l_{\mathbf{X}} - 1))$ -array K such that $K[i, j | l, k] = \langle \Delta \mathbf{x}_{i, t_l}, \Delta \mathbf{x}_{j, t_k} \rangle$ with $i, j \in \{1, \dots, n_{\mathbf{X}}\}$ and $l, k \in \{1, \dots, l_{\mathbf{X}} - 1\}$
 - 2: Initialize an $(n_{\mathbf{X}} \times n_{\mathbf{X}})$ array R with constants σ_0^2
 - 3: Update $R \leftarrow R + \sigma_1^2 \cdot K[:, : | \Sigma, \Sigma]$
 - 4: Initialize an array A with $A \leftarrow K$
 - 5: **for** $n = 2$ to m **do**
 - 6: Perform $A \leftarrow K \odot A[:, : | \boxplus + 1, \boxplus + 1]$
 - 7: Update $R \leftarrow R + \sigma_n^2 \cdot A[:, : | \Sigma, \Sigma]$
 - 8: **end**
 - 9: Return R
-

Algorithm 3 computes the whole covariance matrix $K_{\mathbf{X}\mathbf{X}}$ in $O(n_{\mathbf{X}}^2 \cdot l_{\mathbf{X}}^2 \cdot c + m \cdot n_{\mathbf{X}}^2 \cdot l_{\mathbf{X}}^2)$ time and including intermediary values of a forward pass takes $O(m \cdot n_{\mathbf{X}}^2 \cdot l_{\mathbf{X}}^2)$ memory, which in practice is extensive and quickly becomes a bottleneck. In practice, it is usually not required to compute the inter-dependency structure between the streams, just the diagonals, which is a straightforward modification of the algorithm, and reduces the quadratic cost in $n_{\mathbf{X}}$.

Algorithm 4 is now computed in $O(n_{\mathbf{X}} \cdot l_{\mathbf{X}}^2 \cdot c + m \cdot n_{\mathbf{X}} \cdot l_{\mathbf{X}}^2)$ and the cost in space is $O(m \cdot n_{\mathbf{X}} \cdot l_{\mathbf{X}}^2)$, which is often feasible to compute even at training time due to being able to tune $n_{\mathbf{X}}$ via the minibatch size in the stochastic variational inference procedure.

Algorithm 4: Computing the variances of the GP evaluated at streams $K_{\mathbf{X}} = (\mathbb{E}[f_{\mathbf{x}}f_{\mathbf{x}}])_{\mathbf{x} \in \mathbf{X}}$

Data: Streams $\mathbf{X} = \{\mathbf{x}_1, \dots, \mathbf{x}_{n_{\mathbf{X}}}\} \subset \mathbf{Streams}(W)$, grading vector $\sigma^2 = (\sigma_0^2, \sigma_1^2, \dots, \sigma_m^2)$

Result: Diagonals of the stream-stream covariance matrix $K_{\mathbf{X}} = \text{diag}(K_{\mathbf{X}\mathbf{X}})$

- 1: Compute an $(n_{\mathbf{X}} \times (l_{\mathbf{X}} - 1) \times (l_{\mathbf{X}} - 1))$ -array K such that $K[i|l, k] = \langle \Delta \mathbf{x}_{i,t_l}, \Delta \mathbf{x}_{i,t_k} \rangle$ with $i \in \{1, \dots, n_{\mathbf{X}}\}$ and $l, k \in \{1, \dots, l_{\mathbf{X}} - 1\}$
 - 2: Initialize an $(n_{\mathbf{X}})$ vector R with constants σ_0^2
 - 3: Update $R \leftarrow R + \sigma_1^2 \cdot K[:, \Sigma]$
 - 4: Initialize an array A with $A \leftarrow K$
 - 5: **for** $n = 2$ to m **do**
 - 6: Perform $A \leftarrow K \odot A[:, \boxplus + 1, \boxplus + 1]$
 - 7: Update $R \leftarrow R + \sigma_n^2 \cdot A[:, \Sigma]$
 - 8: **end**
 - 9: Return R
-

6.4 Convergence of the algorithms.

In most benchmarks, we use similar optimization settings. As default, we set $m \leq 5$, that is, we truncate the signature map at degree 5. For the first $n = 1000$ iterations, we fix the kernel hyperparameters and set the learning rate to $\alpha = 1 \times 10^{-3}$. Then unfixing the kernel hyperparameters, we train for another $n = 1000$ iterations, and increase the learning rate to $\alpha = 1 \times 10^{-2}$ for $n = 3000$ iterations, and decreasing it again to $\alpha = 1 \times 10^{-3}$, we finish up by taking $n = 1000$ steps. We tune the learning rate and the number of iterations based on the previous recipe. Particularly, some datasets require to optimize more carefully with fixed $\alpha = 1 \times 10^{-3}$.

In most of our experiments, the sparse VGP with inducing tensors outperforms other VGP variants using signatures. On Figure 1, we can see convergence plots of the ELBO and the testing set accuracy plotted against the time spent optimizing on Arabic Digits, AUSLAN, PenDigits and IMDB. The horizontal axis is the amount of time seconds spent on training the model, including the time spent evaluating the accuracy on test sets every 50 iterations. The test set predictions are computed approximately 100 times even for datasets with more than 1000 testing examples, yet the overall time is still very low. We note that by decreasing m to 3 on IMDB, the overall time reduces to ~ 810 seconds = 13.5 minutes. The convergence is usually smooth, and test set errors closely follow the ELBO, but are apparently not affected by larger oscillations in the ELBO. Overfit does not happen for datasets that are large enough and contain uniform class distributions. We take care when optimizing CMU MOCAP, ECG and KickVsPunch, which are either very small or contain unbalanced classes. In these cases, we optimize carefully and keep the learning rate at $\alpha = 1 \times 10^{-3}$. For two data sets, WalkvsRun and PEMS, our full VGP model without sparsifying the variational approximation but using the low-rank signature kernel as in [20], outperforms the augmented VGP model. On all the other data sets, the augmentation method worked best. On WalkvsRun, convergence to 100% accuracy on the testing set happens in as few as $n = 100$ iterations taking less than 10 seconds.

PEMS is a very high-dimensional dataset with $d = 963$ dimensions, which causes several local optimas and difficulty of optimization. We take two steps to deal with this. Firstly, we enrich streams by dynamically computing their lagged versions for varying lag values via linear interpolation between subsequent observations. This means that we are now dealing with $d = 3852$ dimensional streams per training example, but the same length-scale parameter is applied to all lagged versions of the same coordinate. Adding lags helps in extremely high-dimensional settings to recover length-scale parameters that generalize well, an observation motivated by Taken’s theorem [36]. The lag values are parameters of the embedding from streams to paths, and jointly optimized with other parameters of the model. Additionally, the optimization procedure is highly dependent on initialization, particularly the length-scales. To find good starting values, we split the training set into a smaller set and a validation set, and perform optimization with early termination¹⁰ initializing length-scales randomly on this reduced set, and monitoring the accuracy on the validation set. We repeat such partial trains $k = 3$ times, and choose the length-scales from the best model on the validation set as initial values for optimizing on the complete training set.

¹⁰Typically training for $n = 1000$ iterations this way.

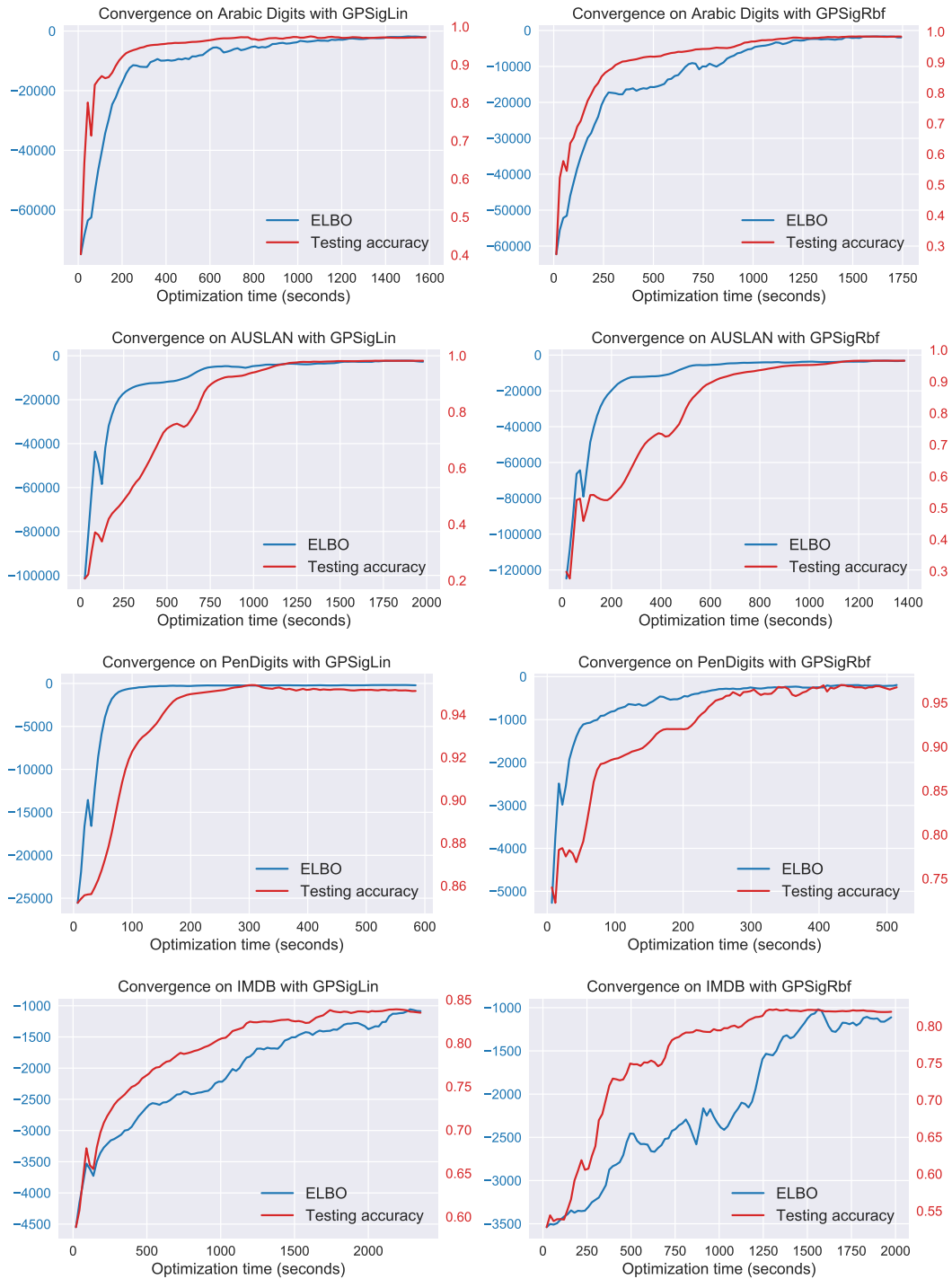


Figure 1: Convergence plots on Arabic Digits, AUSLAN, PenDigits and IMDB. On the horizontal axis visible is the time spent on optimization, blue is the ELBO and red is the testing set accuracy.